



# Dissolved Gas and Metal Composition of Hydrothermal Plumes From a 2008 Submarine Eruption on the Northeast Lau Spreading Center

Tamara Baumberger<sup>1\*</sup>, Marvin D. Lilley<sup>2</sup>, John E. Lupton<sup>3</sup>, Edward T. Baker<sup>4</sup>, Joseph A. Resing<sup>4</sup>, Nathaniel J. Buck<sup>4</sup>, Sharon L. Walker<sup>5</sup> and Gretchen L. Früh-Green<sup>6</sup>

<sup>1</sup> Cooperative Institute for Marine Resources Studies, Oregon State University, Newport, OR, United States, <sup>2</sup> School of Oceanography, University of Washington, Seattle, WA, United States, <sup>3</sup> Pacific Marine Environmental Laboratory, National Oceanic and Atmospheric Administration, Newport, OR, United States, <sup>4</sup> Joint Institute for the Study of the Atmosphere and Ocean, University of Washington, Seattle, WA, United States, <sup>5</sup> Pacific Marine Environmental Laboratory, National Oceanic and Atmospheric Administration, Seattle, WA, United States, <sup>6</sup> Department of Earth Sciences, ETH Zurich, Zurich, Switzerland

## OPEN ACCESS

### Edited by:

Peter R. Girguis,  
Harvard University, United States

### Reviewed by:

Mustafa Yucel,  
Middle East Technical University,  
Turkey  
Shinsuke Kawagucci,  
Japan Agency for Marine-Earth  
Science and Technology (JAMSTEC),  
Japan

### \*Correspondence:

Tamara Baumberger  
tamara.baumberger@noaa.gov

### Specialty section:

This article was submitted to  
Deep-Sea Environments and Ecology,  
a section of the journal  
Frontiers in Marine Science

Received: 24 May 2019

Accepted: 04 March 2020

Published: 24 March 2020

### Citation:

Baumberger T, Lilley MD,  
Lupton JE, Baker ET, Resing JA,  
Buck NJ, Walker SL and  
Früh-Green GL (2020) Dissolved Gas  
and Metal Composition  
of Hydrothermal Plumes From a 2008  
Submarine Eruption on the Northeast  
Lau Spreading Center.  
Front. Mar. Sci. 7:171.  
doi: 10.3389/fmars.2020.00171

Extrusion of lava onto the seafloor transports heat and mass from the lithosphere to the hydrosphere and the biosphere. During this process, large amounts of dissolved gases can be released into the ocean as hydrothermal plumes and serve as nutrients for microbial activity. Here, we report the dissolved gas and metal composition of hydrothermal plumes associated with a submarine eruption at the Northeast Lau Spreading Center (NELSC) in the SW Pacific Ocean in November 2008. During this eruption, two different types of plumes were observed in the water column: a shallow event plume rich in H<sub>2</sub> and poor in <sup>3</sup>He and CH<sub>4</sub>, and a deep near-seafloor plume with high CH<sub>4</sub>, metals and <sup>3</sup>He and intermediate H<sub>2</sub> concentrations. Both were generated at the same time and at the same location. While the high abundance of H<sub>2</sub> in the event plume points to ongoing reactions between hot rock and seawater, the distinct chemical characteristics of the near-seafloor plume likely result from the release of a mature fluid stored in the crust. The plume chemistry of the event plume favors a seawater-lava interaction event plume generation model. However, the heat budget asks for an additional process releasing enough heat to lift the plume within the time frame of this short event. The extremely high H<sub>2</sub> concentrations suggest that the eruption was locally more explosive than assumed. A more explosive eruption style might enhance the heat flux from lava cooling.

**Keywords:** NE Lau Spreading Center, submarine volcanic eruption, hydrothermal plume, dissolved gas, hydrogen, methane, helium, event plume

## INTRODUCTION

Observations of volcanic eruptions in the deep-sea are rare (Rubin et al., 2012). To date, only two submarine volcanoes have been visually observed during an eruption: NW Rota-1 in the Mariana arc (Chadwick et al., 2008) and West Mata in the NE Lau Basin (Resing et al., 2011). Data on real-time characterization of volatiles and metals in hydrothermal plumes associated with seafloor

eruptions is more frequent but still sparse, due both to the rapid consumption of reduced chemical species and short-lived nature of event plumes as well as the limited resources to rapidly respond to eruptions (Baker et al., 1987, 1995a,b; de Angelis et al., 1993; Lilley et al., 1995, 2003; McLaughlin et al., 1996; Kelley et al., 1998; Resing et al., 2007; Baumberger et al., 2014; Chadwick et al., 2018). In particular, H<sub>2</sub> and CH<sub>4</sub> concentration data from young hydrothermal plumes associated with eruptions are very limited (Kelley et al., 1998; McLaughlin, 1998; McLaughlin-West et al., 1999; Resing et al., 2007; Baumberger et al., 2014). In addition, the volatiles released during eruption events drive chemosynthetic ecosystems, and knowledge of the chemical plume composition is relevant for the biosphere. Diverse and abundant microbial populations in event plumes as well as in steady hydrothermal plumes were observed in numerous studies (e.g., Huber et al., 2003; Dick et al., 2013). Processes forming the unique hydrothermal plumes generated by magmatic events are not yet fully understood and different formation hypotheses such as the release of a stored, mature fluid, rapid cooling of a dike intrusion or rapid cooling of a lava flow, have been proposed (Baker et al., 1989, 2011; Baker and Lupton, 1990; Lowell and Germanovich, 1995; Lupton, 1995; Butterfield et al., 1997; Palmer and Ernst, 1998; Lupton et al., 1999, 2000).

The NE Lau region in the South Pacific is a complex tectonic location that combines an arc, backarc and a trench/backarc intersection. This region had been investigated for volcanic and hydrothermal activity prior to 2008 (e.g., German et al., 2006; Kim et al., 2009), but never as systematically as during the NE Lau expedition series starting in 2008 (Baker et al., 2011; Embley et al., 2014). In 2008, extensive hydrothermal event plumes were observed above the neovolcanic zone of the southernmost segment of the Northeast Lau Spreading Center, with the plumes being associated with the “Puipui” eruption (Rubin et al., 2009; Baker et al., 2011). The Puipui flow at the NELSC was visited by the remotely operated vehicle (ROV) *Jason* in 2009 and was described as consisting of highly vesicular basalts in the form of sheet and lobate flows (Clague et al., 2010). Simultaneously, vigorous eruptions were ongoing at the submarine rear-arc volcano West Mata, about 60 km NE of the NELSC (Resing et al., 2011; Baumberger et al., 2014; Embley et al., 2014; Chadwick et al., 2019). The West Mata hydrothermal plume was characterized by exceptionally high dissolved H<sub>2</sub> concentrations and glass shards in the water column indicating reactions between hot rock and seawater (Sansone et al., 1991; Resing et al., 2011; Baumberger et al., 2014).

In this study, we present H<sub>2</sub>, CH<sub>4</sub>, He, Mn, and Fe concentrations and He isotope ratios collected in deep-sea hydrothermal plumes generated during the Puipui eruption at the NELSC (approximately 174.25°W and 15.39°S) in November 2008. The generated plumes were sampled during or within a short time after the eruption of lava on the seafloor. We then compare and contrast our findings with the findings from the simultaneously erupting submarine volcano West Mata (Resing et al., 2011; Baumberger et al., 2014; Embley et al., 2014). These data provide more insights into the properties of young hydrothermal plumes from submarine volcanic eruptions and event plume formation.

## Geological Setting

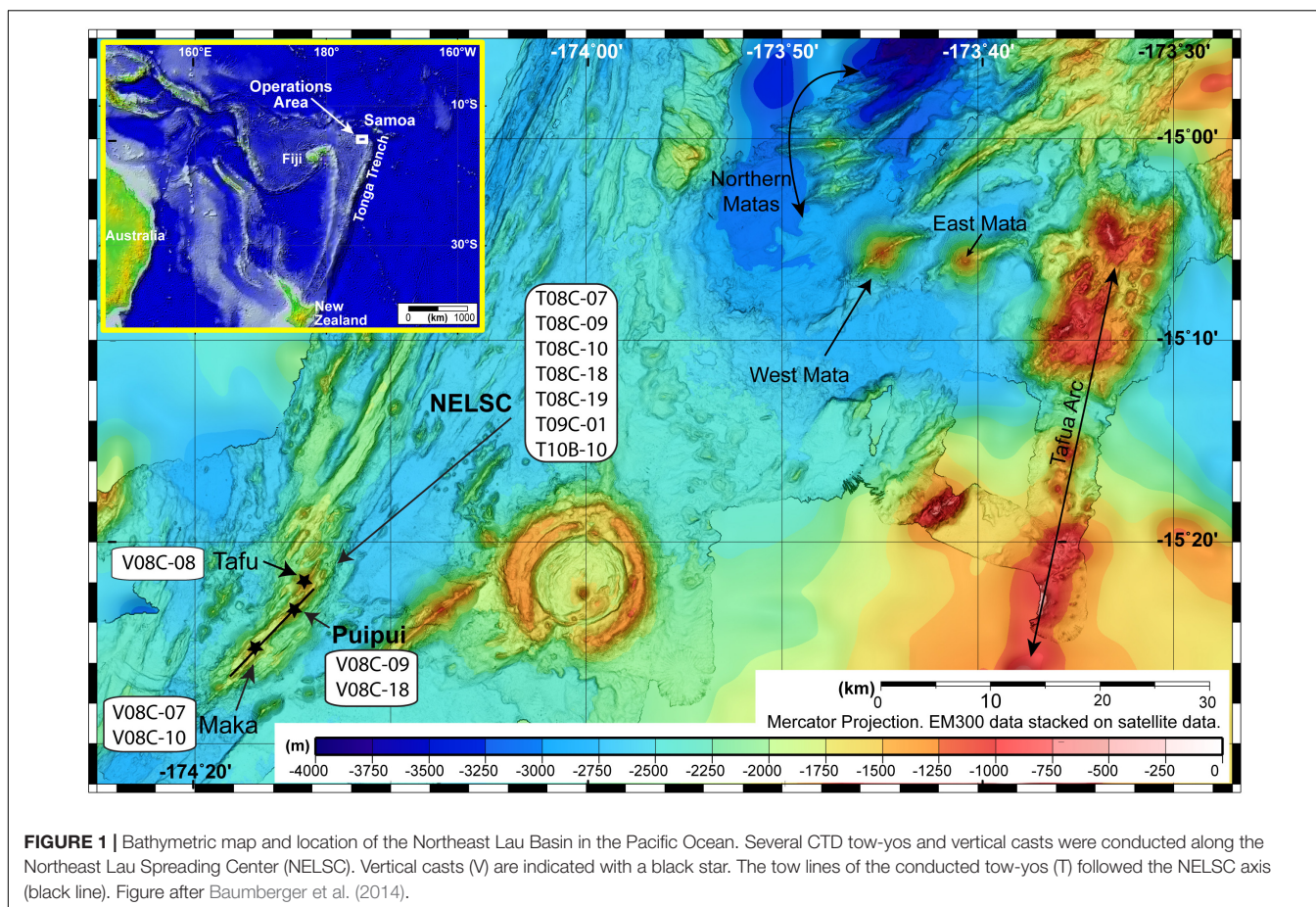
The Northeast Lau back-arc basin is located in the Pacific Ocean SW of the Samoan Islands (**Figure 1**). It is part of the Tonga subduction system, where the Pacific Plate is being subducted westwards beneath the Indo-Australian Plate. The Tonga Trench on the north, the Tofua arc front on the east, and a complex back-arc spreading center system on the west define the Northeast Lau Basin (Hawkins, 1995).

In this paper, we focus on the hydrothermal plumes released during the Puipui eruption located at the NE end of an approximately 15 km long section of the southernmost segment of the NELSC. This section is part of a very complex fast-spreading back-arc spreading center. The spreading rate is believed to be similar to the rate of 85 to 94 mm/yr determined at the NE branch of the nearby Mangatolu Triple Junction (Zellmer and Taylor, 2001; German et al., 2006). This section of the NELSC hosts two known volcanic edifices named Maka and Tafu. Maka is a ridge volcano situated at the southern end of the segment. Several small black-smoker chimneys were observed on the sulfide mound at Maka summit at about 1525 m below sea level during seafloor video surveys in May 2009. Tafu is a ridge volcano northeast of Maka with a summit depth of 1369 m below sea level. Hydrothermal plumes along the southern segment of the NELSC at water depths between 1300 and 1500 m were detected in 2004 (German et al., 2006) and in 2006 (Kim et al., 2009), possibly resulting from Maka or Tafu. Another well-known feature in the NE Lau Basin is the submarine rear-arc volcano West Mata. It is situated about 60 km northeast of the fast-spreading back-arc NELSC, with the Tofua arc front to its east and the westward bending Tonga Trench to its north (**Figure 1**) and a summit depth of 1165 m in 2009. Along the NELSC erupted lavas range from back arc basin basalt (BABB) to basaltic andesite, while West Mata has boninitic magma composition. Multiple other lava flows in the Lau Basin are composed of dacite (Resing et al., 2011; Embley and Rubin, 2018).

## MATERIALS AND METHODS

Most of the data presented here were collected during the *Northeast Lau Basin* cruise on the R/V *Thomas G. Thompson* during expedition TN227 from November 13–28, 2008. Some additional data was collected during the *Northeast Lau Basin Response Cruise* on the R/V *Thomas G. Thompson* (TN234) in May 2009 and during the *2010 NE Lau Basin* expedition on the R/V *Kilo Moana* (KM1008) in April/May 2010.

Plume samples were collected using an instrument package consisting of a Sea-Bird 911 *plus* CTD with an adjunct light scattering sensor (LSS) and an oxidation–reduction potential (ORP) sensor. Water samples were collected using 18.5 L Niskin bottles equipped with Derlin spigots for gas collection and Teflon stopcocks for trace metal sampling. A total of five vertical hydrocasts and seven tow-yos (a sampling technique where the CTD-rosette package is raised and lowered in a saw-tooth like pattern as the ship proceeds on a transect) were conducted to sample and analyze the NELSC plumes and background seawater for <sup>3</sup>He, <sup>4</sup>He, H<sub>2</sub>, CH<sub>4</sub>, TDFe, TDMn, DFe, and DMn.



To determine the dissolved  $\text{H}_2$  and  $\text{CH}_4$  gas concentrations at sea, 100 ml of bubble-free fluid (any air bubbles were removed immediately after drawing the fluid in the syringe) was drawn directly from the Niskin bottle sampling port into 140 ml syringes followed by the addition of 40 ml headspace gas of ultra-pure helium (Kelley et al., 1998). Each sample was vigorously shaken and allowed to warm to room temperature for about 30 min to reach equilibrium for  $\text{H}_2$  and  $\text{CH}_4$  between the water and gas phase. After equilibration, about 20 ml of the headspace gas was injected into a SRI 8610C gas chromatograph through an ascarite/drierite tube trap. Separation of  $\text{CH}_4$  and  $\text{H}_2$  was attained by using a 15 m long Molecular Sieve 5A column. Hydrogen concentrations were determined with a highly sensitive helium-pulsed discharge detector, while  $\text{CH}_4$  concentrations were measured with a flame ionization detector. Both detectors were mounted in series and it was thus possible to measure both,  $\text{CH}_4$  and  $\text{H}_2$  during the same run. Standards were diluted from 100 ppm  $\text{CH}_4$  in He and 100 ppm  $\text{H}_2$  in He from Scotty gas calibration standards. Where sample concentrations exceeded the standard concentrations, samples were diluted to fit the range of the standard curve. The measured background seawater  $\text{H}_2$  and  $\text{CH}_4$  concentrations were  $\sim 0.2$  and  $\sim 0.4$  nM, respectively. The sampling and analytical precision, determined through replicate draws, was about 2.5% of the measured concentrations or  $\pm 0.1$  nM, whichever is greater.

Immediately upon recovery of the underwater sampling package, air-free water samples were flushed through 24-inch-long sections of refrigeration grade Cu tubing with duplicate half-sections cold-weld sealed for later laboratory determinations of He concentration and isotope ratios (Young and Lupton, 1983). Isotope ratios and concentrations of helium were then determined at the NOAA/PMEL Helium Isotope Laboratory in Newport, OR, United States using a dual collector, 21-cm-radius mass spectrometer with  $1\sigma$  precision of 0.2% in  $\delta^3\text{He}$ , where  $\delta^3\text{He}$  is the percentage deviation of  $^3\text{He}/^4\text{He}$  from the atmospheric ratio, and a concentration accuracy of 1% relative to a laboratory air standard. Because helium is a conservative tracer, excess  $^3\text{He}$  is only lost from the ocean by ventilation into the atmosphere at the ocean surface. Consequently, there is a considerable oceanic background level of  $^3\text{He}$ , which has accumulated due to hydrothermal venting. In order to compare  $^3\text{He}$  concentrations against other tracers, we have calculated  $[^3\text{He}]^\Delta$ , which is the  $^3\text{He}$  concentration measured in the hydrothermal plume with the regional background  $^3\text{He}$  concentration subtracted.

Water column samples for total dissolvable Mn and Fe (TDMn and TDFe) were collected directly into 125 ml I-Chem<sup>TM</sup> polyethylene bottles. Dissolved Mn and Fe (DMn and DFe) samples were collected as the filtrate from 0.4  $\mu\text{m}$  acid-washed polycarbonate filters into 125 ml I-Chem<sup>TM</sup> polyethylene bottles after the passage of 2 L of water through the filters. Trace metal

samples were then acidified with 0.5 ml 6N HCl, purified by sub-boiling distillation using a quartz still. Mn was determined with a precision of  $\pm 1$  nM or 4%, whichever is greater, by modifying the direct injection method of Resing and Mottl (1992) by adding 4 g of nitrilo-triacetic acid to each liter of buffer. Fe was determined with a precision of  $\pm 2$  nM by modifying the method of Measures et al. (1995) for direct injection analysis. Background seawater concentrations of Mn and Fe were below detection.

## RESULTS

### Event Plume Chemistry

A table with all measured data can be found in the **Supplementary Material**. The first indication of an on-going eruption at the NELSC was observed on 20 November 2008 in tow-yo T08C-07 at 174.25°W and 15.40°S and at a water depth of 1170 m (**Figure 2** and **Table 1**). An extremely high dissolved H<sub>2</sub> concentration of 6424 nM was measured, which is > 30000 times the concentration seen in local background seawater, while CH<sub>4</sub> showed no enrichment above background and [<sup>3</sup>He]<sup>Δ</sup> was not higher than 0.76 fM, indicating only a small magmatic component. Also on 20 November 2008 we conducted a vertical cast over Maka (V08C-07) and a vertical cast over Tafu (V08C-08) to locate the possible eruption center at the seafloor (**Figures 1, 2**). Both of these stations were over known volcanic cones at the southern segment of the NELSC and both casts showed enhanced H<sub>2</sub> concentrations (Maka: 1962 nM and Tafu: 3040 nM) at water depths between 1010 and 1300 m, but showed no indication for ongoing volcanic eruptions in water samples collected close to the seafloor.

By 21 November 2008, two distinguishable shallow event plume layers were present above the NELSC between 900 and 1500 m water depth (T08C-09, V08C-09, V08C-10) (**Figure 2**; Baker et al., 2011). The upper event plume layer (between 900 and 1300 m water depth) was characterized by very high dissolved H<sub>2</sub> concentrations (**Figure 2** and **Table 1**) up to 9123 nM (T08C-09), comparable to H<sub>2</sub> values of 14840 nM sampled at West Mata volcano during the same cruise (Baumberger et al., 2014) and much higher than measured in other known event plumes (Kelley et al., 1998; McLaughlin-West et al., 1999). Methane concentrations did not exceed 4.6 nM and were only slightly enriched above background seawater values (0.4 nM) measured in the NELSC area. Helium-3 values in the upper layer reached 3.0 fM, about 1.58 fM higher than local background seawater values and low compared to peak concentrations of 5.4 fM measured at the Gorda Ridge in 1996 (Kelley et al., 1998) or 47 fM observed at West Mata (Baumberger et al., 2014). Thus, only small enrichments in <sup>3</sup>He and CH<sub>4</sub> were detected, whereas H<sub>2</sub> concentrations were strongly elevated. TDMn and TDFe concentrations in the upper layer reached 73 and 403 nM, respectively, but were much lower than the highest values (2738 nM TDMn and 5686 nM TDFe) measured in the near seafloor plume at the NELSC (**Table 1**). Over 87% of the TDMn and over 15% of the TDFe were present in the dissolved form.

The lower layer of the event plumes (see **Figure 2**), located between 1300 and 1500 m water depths, exhibited H<sub>2</sub> concentrations similar to the upper layer (up to 9250 nM in V08C-10), whereas methane concentrations were slightly higher (up to 12 nM). The [<sup>3</sup>He]<sup>Δ</sup> concentration was 1.2 fM, again only slightly above background. TDMn values were elevated up to 150 nM and TDFe values up to 465 nM and thus both higher

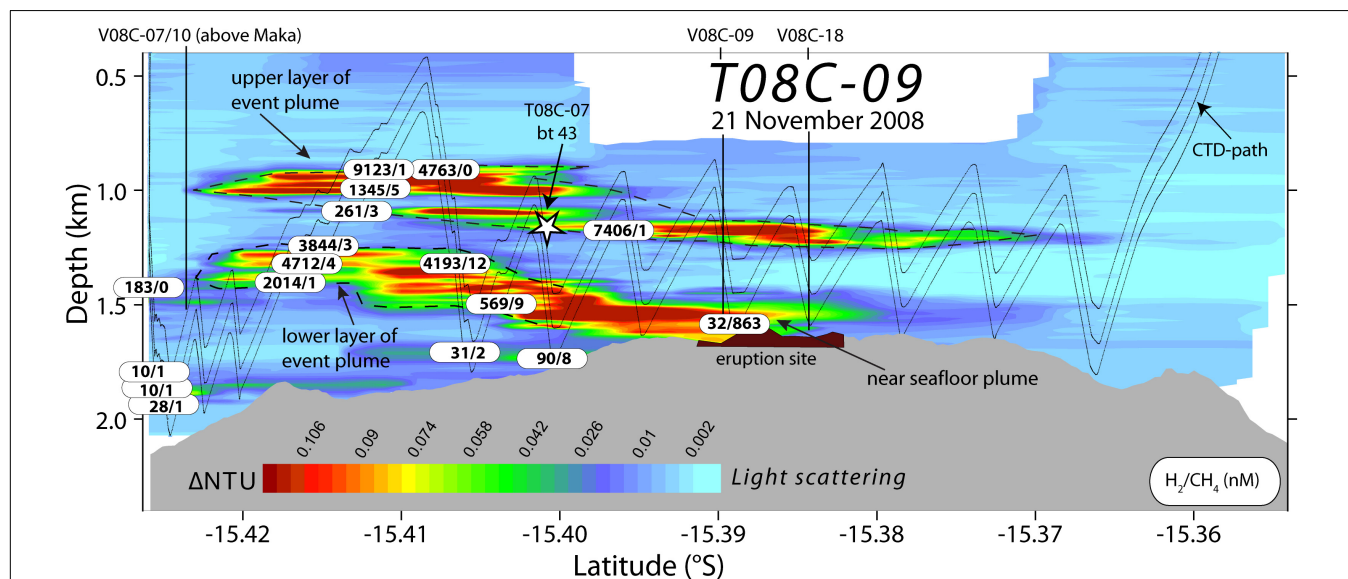


**FIGURE 2** | Water column profile on November 21, 2008 showing particle anomalies of the upper and the lower layer of the event plume and the near seafloor plume. The eruption site is highlighted at the seafloor. The white star indicates position and depth where the first indication of a hydrothermal plume was found on November 20, 2008 in T08C-07 bottle (bt) 43. The black wiggly line shows the CTD-path of T08C-09. Where water samples were taken during this tow, the measured H<sub>2</sub> and CH<sub>4</sub> concentrations are noted in nM at the corresponding location. The locations of the vertical casts are indicated with a black line and cast number. Figure after Baker et al. (2011).

**TABLE 1** | Temporal evolution of the maximum concentrations of H<sub>2</sub>, CH<sub>4</sub>, [<sup>3</sup>He]<sup>Δ</sup>, TDMn and TDFe in the event, near seafloor and deep plumes above the Puipui eruption site.

Plume	H <sub>2</sub> (nM)	CH <sub>4</sub> (nM)	[ <sup>3</sup> He] <sup>Δ</sup> (fM)	TDMn (nM)	TDFe (nM)
<b>Event plume – upper layer</b>					
20 November 2008	6424	0.4	0.76	68	403
21 November 2008	9123	4.6	1.58	73	379
22 November 2008	674	0.4	0.67	39	222
27 November 2008	6.3	0	na	nd	34
08 May 2009	7.7	0.8	na	0	6
<b>Event plume – lower layer</b>					
20 November 2008	Not distinguished from upper layer.				
21 November 2008	9250	12	1.2	150	465
22 November 2008	5082	5.4	0.99	113	361
27 November 2008	2.0	0	na	nd	34
<b>Near seafloor plume</b>					
20 November 2008	No data collected.				
21 November 2008	101	1092	8.50	2738	5686
22 November 2008	74.6	301	2.32	403	1092
27 November 2008	5.5	651	2.23	166	203
06 May 2010	1.7	2.9	na	39	57
<b>Deep plume</b>					
20 November 2008	No data collected.				
21 November 2008	90	8	10.3	199	260
22 November 2008	9.8	0.5	1.64	36	73
27 November 2008	9.3	6.8	7.48	260	298
<b>Background seawater</b>	0.2	0.4	0	0	0

nd, not detected; na, not analyzed.

than in the upper layer (Table 1). Dissolved Mn in the lower layer of the shallow plume reached a percentage of 88 to 100 of the TDMn. Dissolved Fe in the lower layer ranged from 10.7 to 27.2% of the TDFe.

On 22 November 2008, 18 h after T08C-09, T08C-10 was conducted in the same area. Two bottles were triggered in the event plumes, one at 900 m and one at 1350 m (Table 1). Both samples had similar plume chemistry to what was observed 18 h earlier: highly enriched H<sub>2</sub>, enhanced TDMn and TDFe and near background seawater CH<sub>4</sub> and <sup>3</sup>He concentrations, but with lower maximum concentrations.

On 27 November 2008, 7 days after the first surveys, only small H<sub>2</sub> enrichments of 6.3 nM were observed in the area where the event plume had been detected (T08C-18 and T08C-19; Table 1). Thus, the extensive formation of H<sub>2</sub> had ceased and most of the H<sub>2</sub> had been either consumed or advected from the local water column during these 7 days (<sup>3</sup>He data at these depths are not available). The TDFe concentrations were still slightly elevated above background (34 nM), and CH<sub>4</sub> and TDMn concentrations were not distinguishable from background seawater values.

### Near-Seafloor Plume Chemistry

On 21 November 2008, T08C-09 mapped a near-seafloor plume between 1500 and 1620 m centered at 15.389°S (Figure 2 and Table 1). Maximum volatile and metal concentrations were found in vertical cast V08C-09 (about 6 h after T08C-09), approximately

30 m above the seafloor. In this sample we measured 1092 nM CH<sub>4</sub> and 101 nM H<sub>2</sub>. The <sup>3</sup>He concentrations were elevated to 8.5 fM above local background [<sup>3</sup>He (%) = 222] at the same depth. TDMn values were the highest of those sampled at the NELSC (2738 nM) with > 97% of the TDMn present in the dissolved form. TDFe (5686 nM) were also the highest measured along the NELSC with up to 70% in its dissolved form.

Tows conducted over the eruption site over the next 7 days (T08C-10 and T08C-18) and sampling within ~60 m of the seafloor found high CH<sub>4</sub> (up to 651 nM), moderate H<sub>2</sub> (up to 74.6 nM), <sup>3</sup>He (up to 2.23 fM above background) and TDMn (up to 403 nM) and TDFe (up to 1092 nM) values still enriched above background seawater concentrations (Table 1).

### Deep Plume Chemistry

During casts T08C-09, T08C-10 and T08C-18, a plume deeper than the depth of the Puipui lava flow was observed (Table 1). Maximum measured H<sub>2</sub> concentrations in this plume were 90 nM and maximum CH<sub>4</sub> concentrations were 8 nM. This deep plume was characterized by high <sup>3</sup>He concentrations with a <sup>3</sup>He (%) value of up to 255 and [<sup>3</sup>He]<sup>Δ</sup> concentrations of 10.3. Over 97% of the TDMn (74 nM) and up to 75.9% of the TDFe (298 nM) were present in the dissolved form.

### NELSC Plume Chemistry in 2009 and 2010

During the Northeast Lau Basin response cruise 6 months later in May 2009, visual observations by the ROV *Jason* along with water column surveys showed that the eruption at the NELSC had ceased prior to the response cruise. Dissolved H<sub>2</sub>, CH<sub>4</sub>, <sup>3</sup>He, TDFe, and TDMn concentrations measured in the water column above the Puipui lava flow had returned to or near to background values, except for one sample at 1000 m water depth that showed a H<sub>2</sub> value of 7.7 nM (Table 1). By May 2010, when the Puipui lava flow was revisited, only weak H<sub>2</sub>, CH<sub>4</sub>, TDMn, and TDFe enrichments close to the seafloor were found above the zone that was intensively erupting in 2008 (Table 1). Sensors mounted on the CTD did not pick up any anomalies higher up in the water column and consequently no water samples were collected at water depths corresponding to the 2008 event plume layers.

## DISCUSSION

During the 2008 NELSC Puipui eruption, an event plume 200 to 1000 m above the seafloor, a plume near the seafloor eruption and a plume from a source deeper than the Puipui lava flow were observed. The chemistry of these plumes differ from each other as discussed in the following section. We will also compare the plumes associated with the NELSC eruption with those associated with the eruption of the submarine volcanoes West Mata, located 60 km NE of the NELSC, and NW Rota-1 located on the Mariana Arc. We use the data from the NELSC Puipui eruption along with those from other past event plumes, to chemically constrain mechanisms of event plume formation.

## Plume Chemistry and Eruption Modes

Baker et al. (2011) identified the shallow plumes as event plumes. The lowermost layer of the event plumes in T08C-09 intersected with the seafloor, indicating a likely seafloor eruption zone at approximately 15.39°S (Baker et al., 2011). Even though the NELSC eruptions were never visually observed, ROV *Jason* located fresh pillow lava, sheet, and lobate flows as well as vesicular glass fragments and highly degassed pyroclasts during dives at the eruption site in 2009 (Clague et al., 2010). The observed lava flow was named Puipui and had an along-axis extent of about 1.7 km (Clague et al., 2010). The  $^{210}\text{Po}$  activity of three lava samples suggested an eruption in November 2008 (Rubin et al., 2009) that clearly corresponds with our water column observations. To fully exclude Maka as the source of the event plume, we compared the highest  $\text{H}_2/[^3\text{He}]^\Delta$  ratio of the event plumes ( $9152 \times 10^6$ ) with the ratio measured in the Maka end member fluid ( $2.2 \times 10^6$ ). The fact that the  $\text{H}_2/[^3\text{He}]^\Delta$  ratio in the plume is about 4000 times higher excludes the hydrothermal vent field at Maka as a source fluid for the event plume.

The extremely high  $\text{H}_2$  concentrations were a striking feature of the high-rising event plumes at the NELSC and provided strong evidence for on-going or very recent reactions between seawater and molten or extremely hot rock at the seafloor (Figure 2). Extremely high water column  $\text{H}_2$  concentrations were also observed at West Mata during the same cruise (Baumberger et al., 2014) and in May 2009, when concurrent visual observations of ongoing eruptions and  $\text{H}_2$  measurements in the water column and of the fluids close to erupting lava at the seafloor confirmed the relationship between eruption and the production of  $\text{H}_2$  (Resing et al., 2011; Baumberger et al., 2014). By comparison,  $\text{H}_2$  concentrations obtained from event plume EP96A at the Gorda Ridge in 1996, reached a maximum of 47 nM (Kelley et al., 1998). The differences in  $\text{H}_2$  concentrations are at least partially due to the time elapsed after eruption, as chemical aging of EP96A had already begun when the plume was sampled (Kelley et al., 1998). At the NELSC, between 11 and 29% of the total Fe ( $\text{TDFe}_{\text{max}} = 465 \text{ nM}$ ) in the event plumes was present in its dissolved form on November 21, 2008 indicating that these plumes were less than 1 day old when sampled, assuming a Fe oxidation half-time in the Pacific between 2 and 6 h (Field and Sherrell, 2000). In the same  $\text{H}_2$ -rich event plumes,  $\text{CH}_4$  values did not exceed 12 nM. This suggests that during the  $\text{H}_2$ -producing processes, the production of  $\text{CH}_4$  is almost negligible and therefore  $\text{CH}_4$  is not generated in significant quantities during reactions between hot rock and seawater, at either quiescent lava flows or from explosive volcanic eruptions. This trend has also been observed at other volcanoes that were sampled while erupting or while in early stage of post-eruption evolution, such as West Mata (Baumberger et al., 2014), NW Rota-1 (Resing et al., 2007; Butterfield et al., 2011), Gorda Ridge in 1996 (Kelley et al., 1998), along the coastline of Kilauea Volcano when lava enters the ocean (Sansone et al., 1991; Sansone and Resing, 1995) and more recently at Ahyi seamount (Buck et al., 2018). Significantly higher  $\text{CH}_4$  concentrations of 522 nM were measured in a possible, but not confirmed event plume at Axial Volcano 18 days after an eruption in 1998 (McLaughlin-West et al., 1999;

Baker et al., 2011). The  $\text{CH}_4$  values in the shallow NELSC event plume layers were poorly correlated with  $\text{H}_2$  and  $^3\text{He}$ . Juvenile carbon and inorganic  $\text{CH}_4$  synthesis as a source for the slight  $\text{CH}_4$  enrichment in the shallow event plume layers is unlikely because a good correlation with  $^3\text{He}$  would be expected, at least close to the eruption site (Welhan, 1988; Mottl et al., 1995). Methane can originate from microbial production in a more evolved system, where hydrothermal fluid stored at depth can be released during magmatic eruptions as some models for event plume formation suggest (Baker and Lupton, 1990; Lupton et al., 1995; Butterfield et al., 2004; Von Damm and Lilley, 2004). In this scenario, higher  $\text{CH}_4$  concentrations and a higher degree of correlation with  $^3\text{He}$  would be expected in the plume. The most likely source for  $\text{CH}_4$  in the event plume layers is thermogenically degraded organic matter caused by hot lava enveloping biological communities (Welhan, 1988). Although the presence of a lava flow was confirmed in 2009 by video images, there is no information regarding preexisting biological communities at this site.

In contrast to the low  $\text{CH}_4$  concentrations in the event plume, high  $\text{CH}_4$  concentrations were detected in the near seafloor plume close to the Puipui eruption zone (Figure 2 and Tables 1, 2). Methane and  $^3\text{He}$  were well-correlated with  $\text{CH}_4/[^3\text{He}]^\Delta = 122 \times 10^6$  ( $r^2 = 0.87$ ). This ratio is 6 to 1200 times higher than in the event plume. In addition,  $\text{CH}_4$  is well-correlated with TDMn ( $r^2 = 0.91$ ) and TDFe ( $r^2 = 0.91$ ). The excellent correlations between  $\text{CH}_4$ ,  $^3\text{He}$ , TDFe, and TDMn suggest that we sampled a young plume that had experienced limited oxidation. Dissolved Fe in hydrothermal vents is typically in its reduced form. It has been thought from earlier studies that iron dissolved in a hydrothermal plume oxidizes within hours, rapidly forming particulates (Field and Sherrell, 2000). More recent studies suggest that stabilization of dissolved iron in the hydrothermal plume results in transportation of dissolved iron over long distances at near conservative behavior (Bennett et al., 2008; Sander and Koschinsky, 2011; Yücel et al., 2011; Resing et al., 2015). However, rapid oxidation and loss of hydrothermal Fe from the dissolved phase close to the eruption center is still valid (Resing et al., 2015). Thus, dissolved Fe reaching up to 70% of the TDFe in the near seafloor plume confirms a young age of the plume. Furthermore, ratios of  $\text{CH}_4$  relative to  $^3\text{He}$ ,  $\text{H}_2$  and TDMn clearly distinguish the event plume layers from the near seafloor plume (Table 2). Hydrogen/ $\text{CH}_4$  ratios are up to 1200 times smaller than in the event plume and require a  $\text{CH}_4$ -rich source. The elevated  $\text{H}_2$  in the event plume layers and the high  $\text{CH}_4$  in the near-seafloor plume likely have distinct fluid sources and reflect different fluid evolution processes. A likely source for the near seafloor plume is the release of a stored, mature hydrothermal fluid containing microbial  $\text{CH}_4$  and likely triggered by the eruption. Methane/TDMn ratios in the near seafloor plume were between 0.4 and 0.8 and fall in the range typical for magmatic degassing, bacterial production or the reaction between seawater and basalt as  $\text{CH}_4$  sources (Mottl et al., 1995). Bacterial production is in agreement with the release of a pre-stored fluid as a likely  $\text{CH}_4$  source. Manganese concentrations in hydrothermal fluids are reflective of two main factors: the ratio of water to rock and the length of

**TABLE 2** | Summary of temporal evolution of geochemical ratios in the Puipui event and near seafloor plumes compared to geochemical ratios observed in other event and volcanic eruption plumes.

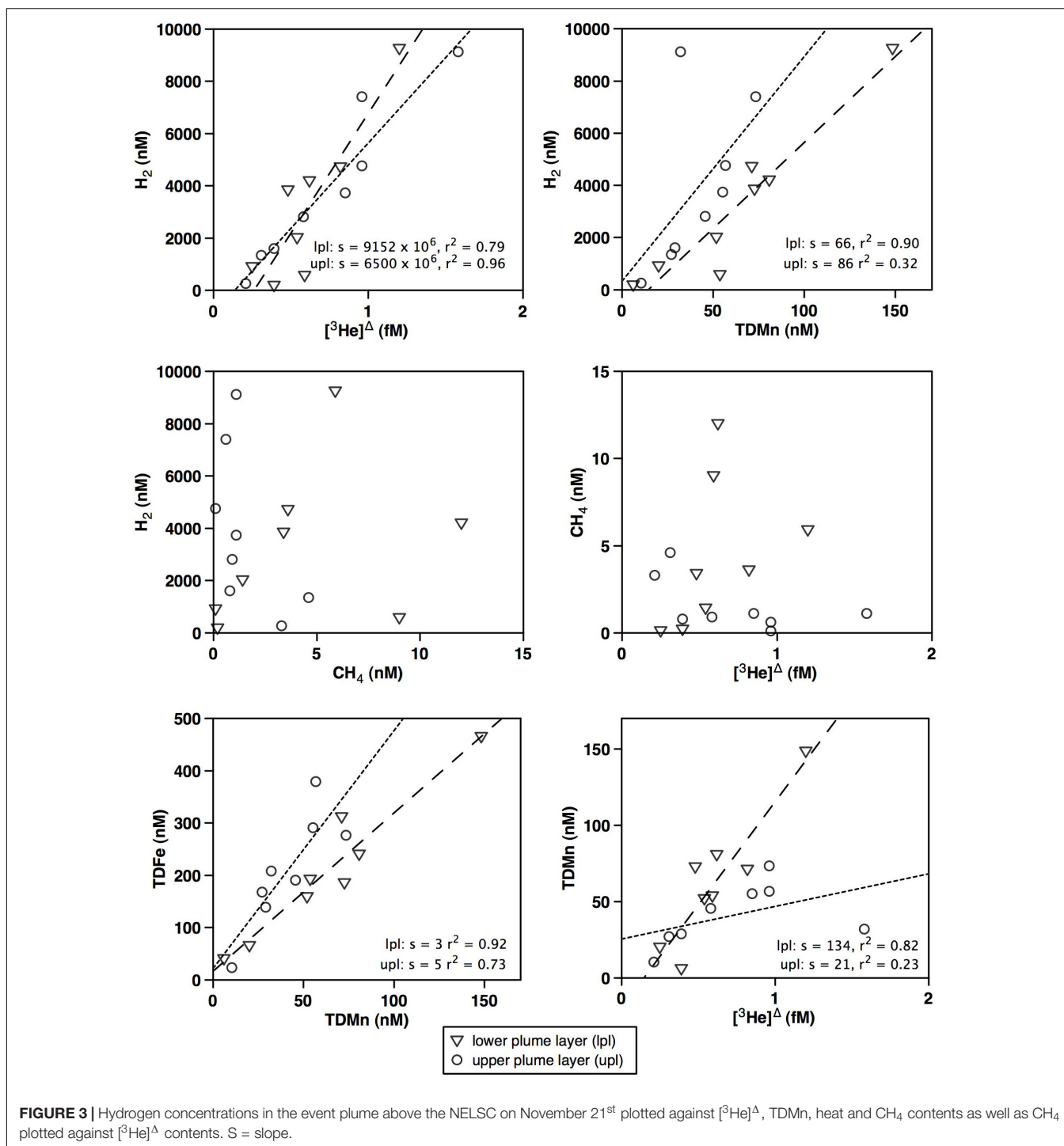
	$H_2/[^3He]^A$ $\times 10^6$	$CH_4/[^3He]^A$ $\times 10^6$	$H_2/CH_4$	$H_2/TDMn$	$CH_4/TDMn$	$TDMn/[^3He]^A$ $\times 10^6$	$TDFe/TDMn$	References
<b>NELSC 2008</b>								
<i>November 20</i>								
Event plume	8453 <sup>b</sup>	0.5 <sup>b</sup>	16060 <sup>b</sup>	94.5 <sup>b</sup>	0.006 <sup>b</sup>	90 <sup>b</sup>	5 <sup>b</sup>	This study
<i>November 21</i>								
Upper plume layer	6500 (0.92) <sup>a</sup>	0.1 to 16 <sup>c</sup>	79 to 47631 <sup>c</sup>	86 (0.32) <sup>a</sup>	0.01 to 0.32 <sup>c</sup>	21 (0.23) <sup>a</sup>	5 (0.73) <sup>a</sup>	This study
Lower plume layer	9152 (0.79) <sup>a</sup>	0.5 to 19 <sup>c</sup>	63 to 9026 <sup>c</sup>	66 (0.90) <sup>a</sup>	0.03 to 0.17 <sup>c</sup>	134 (0.82) <sup>a</sup>	3 (0.92) <sup>a</sup>	This study
Near seafloor plume	8 (0.56) <sup>a</sup>	122 (0.87) <sup>a</sup>	0.05 (0.31) <sup>a</sup>	0.02 (0.56) <sup>a</sup>	0.4 (0.91) <sup>a</sup>	336 (0.99) <sup>a</sup>	2 (1.00) <sup>a</sup>	This study
<i>November 22</i>								
Upper plume layer	1002 <sup>b</sup>	0.6 <sup>b</sup>	1685 <sup>b</sup>	17 <sup>b</sup>	0.01 <sup>b</sup>	58 <sup>b</sup>	6 <sup>b</sup>	This study
Lower plume layer	5150 <sup>b</sup>	5.5 <sup>b</sup>	941 <sup>b</sup>	45 <sup>b</sup>	0.05 <sup>b</sup>	115 <sup>b</sup>	3 <sup>b</sup>	This study
Near seafloor plume	10 to 43 <sup>c</sup>	44 to 227 <sup>c</sup>	0.2 to 0.7 <sup>c</sup>	0.1 to 0.2 <sup>c</sup>	0.3 to 0.9 <sup>c</sup>	203 (0.94) <sup>a</sup>	3 (0.88) <sup>a</sup>	This study
<i>November 27</i>								
Upper plume layer	nd	nd	nd	nd	nd	nd	nd	This study
Lower plume layer	nd	nd	nd	nd	nd	nd	nd	This study
Near seafloor plume	4 <sup>b</sup>	130 <sup>b</sup>	0 <sup>b</sup>	0.03 <sup>b</sup>	0.5 <sup>b</sup>	271 <sup>b</sup>	1 <sup>b</sup>	This study
<b>Other plumes</b>								
West Mata November 2008	425	0.2 to 3.5	35 to 3452	26	0.02	22	8	Baumberger et al., 2014
NW Rota-1	nd	0.1 to 0.4	nd	nd	0.014	9.8	14	Resing et al., 2007, 2009
Plume Axial Volcano	nd	17 to 37	nd	nd	2.2	8.5 to 15	nd	McLaughlin-West et al., 1999
Gorda plume EP96A	20.9	3.2	nd	0.8	0.11	29	nd	Kelley et al., 1998
Gorda plume EP96B	4.9	2.3	nd	0.2	0.10	23	nd	Kelley et al., 1998
Cleft Event Plume 1986	nd	nd	nd	nd	0.3	nd	nd	Kelley et al., 1998

nd = not determined. <sup>a</sup>Ratios derived from regressions of all samples collected in the corresponding plume layer at the reported time. R-squared values given in brackets. <sup>b</sup>Calculated ratio from one available sample in the corresponding plume layer at the reported time. <sup>c</sup>Calculated ratios from a range of samples in the corresponding plume layer at the reported time with an R-squared of linear regression line < 0.20.

the water-rock reaction pathway within the magma chamber (Bowers et al., 1988). An Fe/Mn ratio of 2 in the near seafloor plume is at the low end of the typical range (Fe/Mn = 1 to 5) for mid-ocean ridge hydrothermal fluids (e.g., Von Damm, 1990), possibly due to the longer reaction time between host rock and fluid in a mature system. A hydrothermal plume close the seafloor was observed at Axial Seamount in the Northeast Pacific after the 2015 eruption (Xu et al., 2018). Numerical modeling supports the hypothesis that the 2015 Axial eruption triggered the release of warm brines and that these formed the observed plume near the seafloor. In contrast, density, temperature, and salinity data collected in the NELSC near-seafloor plume point to a buoyant plume and the release of a fluid with different chemistry.

The  $\delta^3He$  values measured in the  $H_2$ -rich and  $CH_4$ -poor event plume were lower than the  $\delta^3He$  values in the more mature near seafloor plume. Primordial  $^3He$  is released from the Earth's interior through volcanic processes. Because of its conservative behavior in marine geochemical and biological processes,  $^3He$  in a hydrothermal plume is only reduced by dilution. Ratios of  $H_2/[^3He]^A$  in hydrothermal plumes are thus a function of source composition and plume age. At the NELSC,  $H_2/[^3He]^A$  ratios of both layers of the event plume on 21 November, 2008 were in the same range and  $H_2$  and  $[^3He]^A$  were well-correlated with each other (Figures 3, 4 and Table 2). The stronger correlation of the upper layer might be caused by spatial and temporal

differences in  $H_2$  production during the reaction of molten rock with seawater (Baker et al., 2011). The  $H_2/[^3He]^A$  ratios in the event plume were substantially higher (up to  $9152 \times 10^6$ ) than in the near seafloor plume and in the axial plumes originated deeper than the eruption site. In addition,  $H_2/[^3He]^A$  ratios in the event plume at the NELSC were 100 times higher than ratios detected in hydrothermal event plumes after eruptions studied previously at other sites (Kelley et al., 1998; McLaughlin-West et al., 1999). The high  $H_2/[^3He]^A$  ratios are not only a result of age difference compared to previously studied plumes, but also due to the extraordinary high levels of  $H_2$  and weak  $^3He$  signals observed in the event plume at the NELSC. In fact, based on  $^3He$ /heat ratios, the  $^3He$  load in the NELSC event plume was only 20 to 25% of the load observed at other event plume sites (Baker et al., 2011). Elevated  $H_2$  is the result of extensive production during hot rock – seawater interaction, while the comparatively low  $^3He$  concentrations indicate a small magmatic contribution to the event plume (Baker et al., 2011). On 22 November,  $H_2/[^3He]^A$  ratios were  $1002 \times 10^6$  (900 m) and  $5150 \times 10^6$  (1350 m), respectively (Table 2). Both ratios decreased significantly within 18 h, which suggests that  $H_2$  oxidation started to affect the concentration measurements of the first plumes and dilution cannot be the only reason for the lower  $H_2$  concentrations (McLaughlin et al., 1996). Abiotic oxidation and biological uptake are possible pathways for  $H_2$  removal (e.g., McCollom and Shock, 1997; McCollom, 2000; Dick, 2019). Due

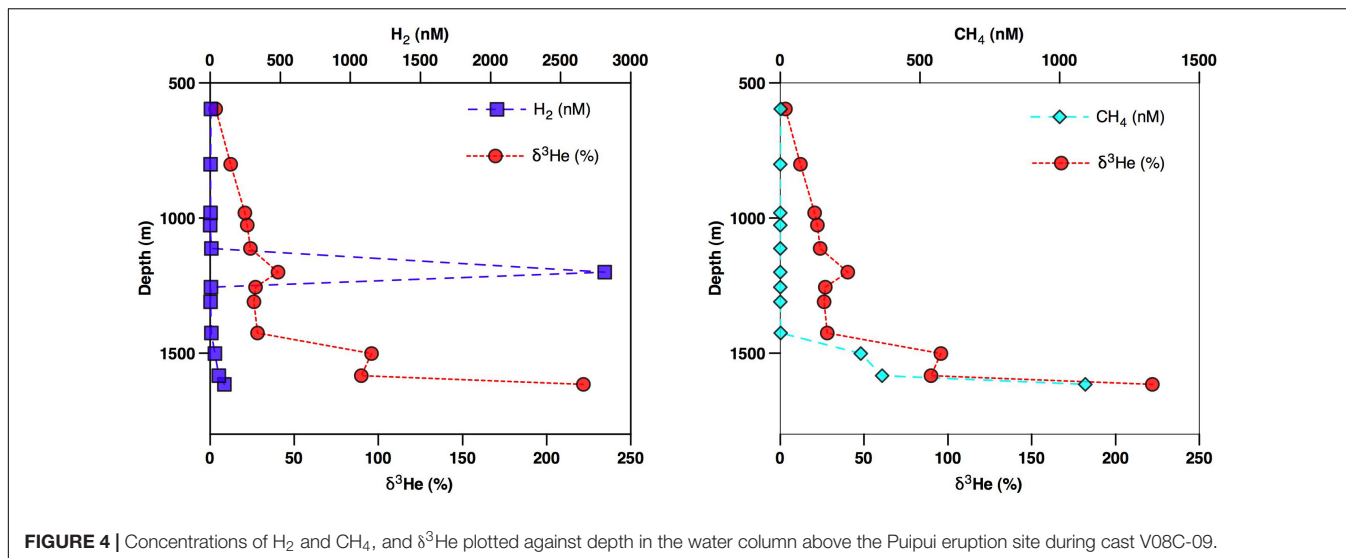


to the high  $\text{H}_2$  availability in the event plume,  $\text{H}_2$ -oxidizers could grow rapidly and consume the abundant  $\text{H}_2$  quickly, in addition to ongoing chemical oxidation. This is consistent with the dramatic decrease of  $\text{H}_2$  concentrations and  $\text{H}_2/[^3\text{He}]^\Delta$  ratios within 18 h observed here at the NELSC. Such volcanic events can thus significantly enhance the locally available catabolic energy in the water column and potentially cause a post-eruption microbial bloom of  $\text{H}_2$  oxidizers (Amend et al., 2011). Anantharaman

et al. (2013) suggest that microbial  $\text{H}_2$  oxidation can be a key energy source in the deep ocean. Seven days after the first  $\text{H}_2$  measurements in the event plume, concentrations were decreased by a factor of 1000 to about 10 to 15 times above background concentrations. A microbial bloom of  $\text{H}_2$  oxidizers generated by an event plume would thus last for only a short time.

**Figure 5** shows distinct  $\text{H}_2/[^3\text{He}]^\Delta$  relationships in the NELSC event plumes, the NELSC near seafloor plume, and





the hydrothermal plume above the erupting submarine volcano West Mata (Baumberger et al., 2014). The ratios of the three plumes are clearly distinguishable. The slope representing the high H<sub>2</sub>/[<sup>3</sup>He]<sup>Δ</sup> ratio in the event plume is very steep. The comparatively low H<sub>2</sub> and high <sup>3</sup>He concentrations found in the near seafloor plume result in a flat slope. At West Mata, H<sub>2</sub>/[<sup>3</sup>He]<sup>Δ</sup> ratios were characterized by high H<sub>2</sub> and high <sup>3</sup>He concentrations at the time of sampling and were thus intermediate between the two types observed at the NELSC. These ratios represent the prevailing processes at the different sites. At West Mata, small, almost continuous submarine volcanic eruptions with hot rock-fluid interactions and concurrent release of magmatic volatiles are prominent. At the NELSC, two different processes may be responsible for the striking H<sub>2</sub>/[<sup>3</sup>He]<sup>Δ</sup> pattern. High ratios in the event plume derive from H<sub>2</sub> generation during

hot rock and seawater interactions induced by a relatively large lava flow accompanied by a decoupled release of <sup>3</sup>He. Hydrogen was produced at the eruptive fissure and along the whole lava flow as long as seawater was in contact with hot lava, while some low-level degassing of <sup>3</sup>He likely caused the small <sup>3</sup>He elevations in the event plume. It is thought that <sup>3</sup>He and other primordial gases separate from the magma in the magma chamber and that these gases are released in excess upon eruption (Graham et al., 2018). Most of the <sup>3</sup>He may have degassed during the initial rise of the magma and/or when the magma exited from the seafloor leading to a spatial and temporal separation of <sup>3</sup>He degassing and H<sub>2</sub> production.

The deep plume observed in the same time frame as the event plume layers and the near seafloor plume have a typical high temperature hydrothermal vent composition and indicate venting of a fluid from an edifice located deeper than the ongoing lava eruption. No such hydrothermal vent system was located during the 2009 ROV dives. However, the dives were mainly focused on the Puipui flows and on Maka and may have missed the remains of such a system.

### Comparison of the NELSC With the West Mata and NW Rota-1 Eruptions

Table 3 is a summary of the main characteristics of the NELSC Puipui, West Mata and NW Rota-1 eruptions. The West Mata and NW Rota-1 eruptions were both observed visually, are located close to a volcanic arc and have an explosive/strombolian eruption type. In contrast, the Puipui lava flow erupted on a back-arc spreading center. The Puipui NELSC lava eruption and the eruption of West Mata were both ongoing during the same time in November 2008. Both were initially identified by very high H<sub>2</sub> concentrations measured in the water column above the eruption sites. At West Mata, the enormous H<sub>2</sub> enrichments resulted from water/rock interactions during gas-rich eruptions accompanied by quiet, degassed outflow of magma forming pillow lava as observed by ROV *Jason* in May 2009 (Resing et al., 2011;

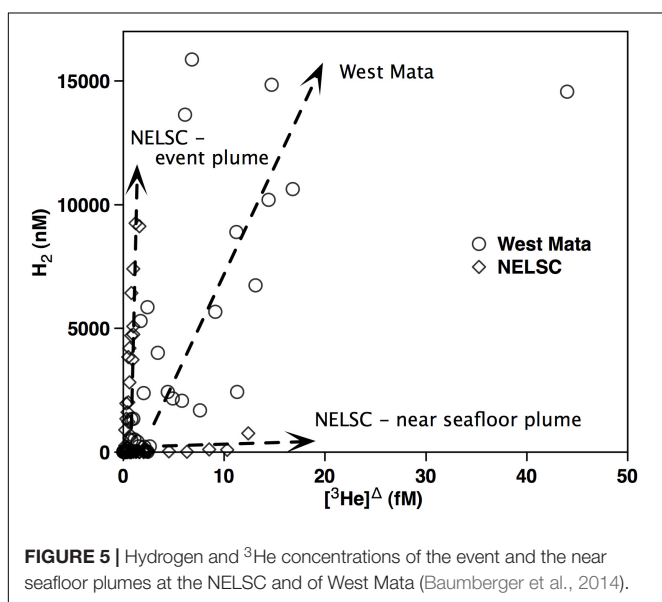


**TABLE 3** | Comparison of geochemical data and other characteristics of the NELSC plumes, the West Mata plume and the NW Rota-1 plume.

Site	NE Lau Spreading Center			West Mata	NW Rota-1
<b>References</b>	This study; Baker et al., 2011; Embley and Rubin, 2018			Resing et al., 2011; Baumberger et al., 2014; Embley et al., 2014	Resing et al., 2007, 2009; Chadwick et al., 2008; Stern et al., 2008
<b>Plume type</b>	<b>Event plume</b>	<b>Near-seafloor plume</b>	<b>Deep plume</b>	<b>Focused plume</b>	<b>Focused plume</b>
Geological setting	Back-arc	Back-arc	Back-arc	Rear-arc	Arc
Eruption type	Short-lived, explosive?	Effusive?	Effusive	Explosive/strombolian	Explosive/strombolian
Time-frame eruption	Event	Event?	Event?	Continuous	Continuous
Chemical character plume	Rich in H <sub>2</sub> , poor in <sup>3</sup> He	Rich in CH <sub>4</sub> and <sup>3</sup> He	Rich in <sup>3</sup> He	Rich in <sup>3</sup> He, H <sub>2</sub> , S, CO <sub>2</sub>	Rich in Al, S, Si, CO <sub>2</sub> , Fe, Mn, <sup>3</sup> He, acid
Max H <sub>2</sub> measured (nM)	9250	101	90	14843	Not measured
Max CH <sub>4</sub> measured (nM)	12	1092	8	10	5
Max TDMn measured (nM)	150	2738	74	359	150
Max % DMn	100	100	99.9	>95	>95
Max TDFe measured (nM)	465	5686	298	3275	2300
Max % DFe	72.2	69.7	39.7	11	<10
Max δ <sup>3</sup> He (%)	67.5	222	255	442	314
Max [ <sup>3</sup> He] <sup>Δ</sup> measured (fM)	1.6	8.5	10.4	47	15.3
H <sub>2</sub> /[ <sup>3</sup> He] <sup>Δ</sup> (x 10 <sup>6</sup> )	9152	43	13.2	2839	No H <sub>2</sub> measured
CH <sub>4</sub> /[ <sup>3</sup> He] <sup>Δ</sup> (x 10 <sup>6</sup> )	19	227	1	0.3	0.3
H <sub>2</sub> /CH <sub>4</sub>	47631	0.7	13.7	2370	No H <sub>2</sub> measured
Estimated R/Ra	7.9 to 8.6	8	Not Determined	7.2	8.4
Plume rise height (m)	200 to 1000	<30 to 130	Unknown	130	100
Glass shards in plume	Yes	No	No	Yes	Yes
Bubble plume	No	No	No	No	Yes
Lava type	Basalt, basaltic andesite	Basalt, basaltic andesite	Basalt, basaltic andesite	Boninite	Basalt, basaltic andesite, andesite

Baumberger et al., 2014). In contrast to the size of the volcanic eruption at West Mata where explosive deposits and pillow flows formed in a restricted area, the high H<sub>2</sub> concentrations at the NELSC eruption resulted from water/rock interactions of a lava flow extending about 1.7 km along the ridge axis (Rubin et al., 2009; Resing et al., 2011). Despite this difference in size, the maximum measured H<sub>2</sub> concentrations in both plumes are in a comparable range and probably result from explosive eruption activity. Hydrogen concentrations were not analyzed in the NW Rota-1 plume and we thus have no information as to whether the NW Rota-1 plumes were rich in H<sub>2</sub>. Maximum measured CH<sub>4</sub> concentrations are low in the NELSC event plume as well as in the two plumes generated from the continuous explosive eruptions at West Mata and NW Rota-1. This confirms that CH<sub>4</sub> plays only a minor role in the formation of high rising plumes from submarine volcanic eruptions and lava outflows. The <sup>3</sup>He patterns are less uniform over the three eruption sites. Whereas low <sup>3</sup>He input in event plumes has been observed during several historical events (with the NELSC event plume having the lowest input), both volcanic eruptions, West Mata and NW-Rota-1, are rich in mantle helium and have a continuous supply of magmatic gas input (Resing et al., 2007; Baker et al., 2011; Butterfield et al., 2011; Baumberger et al., 2014). The NELSC event plume as well as the focused plumes from the two volcanic

eruptions have variable TDMn/DMn ratios, likely resulting from the different plume ages sampled. In contrast, the near seafloor plume at the NELSC has highly elevated CH<sub>4</sub>, TDMn, and TDFe contents with the high percentage of dissolved Fe pointing to a very young plume. Despite similarities in volcanic activities, TDFe/TDMn ratios in the NW Rota plume (TDFe/TDMn = 14) were considerably higher than at West Mata (TDFe/TDMn = 8) and in the NELSC event plumes (TDFe/TDMn = 3–6). At NW Rota, venting of highly acidic fluids likely causes dissolution of the host rock resulting in fluids with higher TDFe/TDMn ratios closer to the host rock (Resing et al., 2007). Acidic fluids were also reported at West Mata (Resing et al., 2011). However, the short reaction time with the host rock during the ongoing eruptions as well as the boninite magma composition likely lead to lower ratios than observed at NW Rota. In contrast, the NELSC plumes are more similar to the low Fe/Mn hydrothermal systems found on mid-ocean ridges.

To determine the role of the geological setting for the magmatic gas source during these three eruptions, we use helium isotope ratios. The <sup>3</sup>He/<sup>4</sup>He helium isotope ratio R/R<sub>a</sub>, where  $R = \frac{{}^3\text{He}}{{}^4\text{He}}$  and  $R_a = R_{\text{air}} = 1.39 \times 10^{-6}$  (Graham, 2002), can be used to obtain information about the source of the helium. This is especially useful in complex tectonic settings, such as arc-backarc settings or where hot spots are nearby. The R/R<sub>a</sub>

of the upper mantle is  $8.0 \pm 1$  based on values observed in MOR basalts and hydrothermal fluids (Poreda and Craig, 1989; Graham, 2002).  $R/R_a$  ratios at volcanic arcs are about 5 to 7, generated by a mixture of mantle helium and slab material that is relatively enriched in  $^4\text{He}$  (Hilton et al., 2002). The  $^3\text{He}/^4\text{He}$  ratios are usually determined from direct measurements in end member fluids collected at the seafloor. Where direct sampling of seafloor vent or eruption fluids is not possible, dilute water column samples can be used to estimate  $^3\text{He}/^4\text{He}$  ratios in the end member fluid erupted at the seafloor (Lupton et al., 2015). We used the vertical cast V08C-09, collected over the Puipui eruption site, to estimate the end member  $R/R_a$  value of the near seafloor plume by plotting  $^3\text{He}$  vs.  $^4\text{He}$  concentrations of both, the plume and the background concentrations. The resulting slope corresponds to the  $^3\text{He}/^4\text{He}$  ratio =  $R$ . We estimated an  $R$  value of  $8.0 R_a$  for the near seafloor plume, which falls in the MORB field (Figure 6). We did the same exercise with the event plume and estimated an  $R/R_a = 8.6$  for the upper layer and  $R/R_a = 7.9$  for the lower layer. These ratios correspond well with the measured  $^3\text{He}/^4\text{He}$  ratios in the high temperature end member vent fluids at Maka located on the NELSC ( $8.7 R_a$ ), and the ratio measured in fluids from a diffuse vent site ( $8.0 R_a$ ) located on the SW-NELSC (Lupton et al., 2015). As expected from the geological setting of the back-arc spreading center, the established NELSC hydrothermal vent fields as well as the recent Puipui eruption have the upper mantle as their main helium source, similar to mid-ocean ridges, and are apparently not impacted by the Samoan hot spot, nor by the volcanic arc, which is in good agreement with Lupton et al. (2015). In contrast,  $^3\text{He}/^4\text{He}$  ratios of the rear-arc volcano West Mata, erupting at the same time 60 km NE of the NELSC, had an estimated ratio of  $7.2 R_a$  and arc-like  $^3\text{He}/^4\text{He}$ - $\text{C}/^3\text{He}$  attributes (Lupton et al., 2015). At NW Rota-1, despite being an arc volcano, the upper mantle was the main source for its helium ( $R = 8.4 R_a$ ; Resing et al., 2009), possibly reflecting source heterogeneity within small distances as observed in the Manus Basin (Fourre et al., 2006).

## Chemical Constraints on Event Plume Formation

Baker et al. (1987) described the first discovery of an event plume, or megaplume, on the Cleft segment of the southern Juan de Fuca Ridge in 1986. They reported the formation of an extensive plume of a thickness of 700 m and a diameter of 20 km created by a brief and massive release of high-temperature hydrothermal fluid (Lupton et al., 1989; Baker and Lupton, 1990). Another event plume with heat and chemical anomalies was discovered above the North Fiji Basin in 1987, a very different tectonic environment compared to the Juan de Fuca Ridge (Nojiri et al., 1989). In 1993, a series of event plumes, with plume volumes from  $1.3$  to  $4 \times 10^{10} \text{ m}^3$  was observed above the CoAxial segment of the Juan de Fuca Ridge (Baker et al., 1995b; Embley et al., 1995; Lupton et al., 1995). After the remote detection of seismic swarms, event plumes above the northern Gorda Ridge were also observed during quick response cruises in 1996. There, a major event plume was detected rising nearly 1500 m with a thickness of approximately 1 km and an extension of 15 km along and at

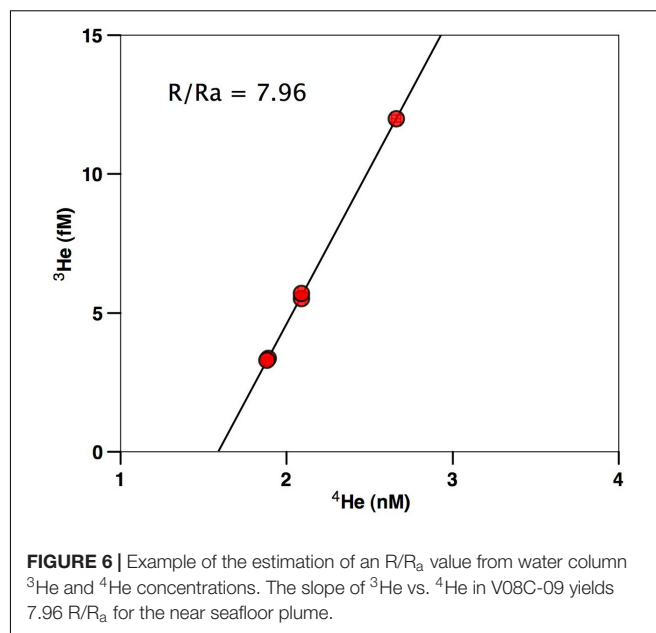


**FIGURE 6** | Example of the estimation of an  $R/R_a$  value from water column  $^3\text{He}$  and  $^4\text{He}$  concentrations. The slope of  $^3\text{He}$  vs.  $^4\text{He}$  in V08C-09 yields  $7.96 R/R_a$  for the near seafloor plume.

least 8 km across axis (Baker, 1998). However, dissolved  $\text{H}_2$  and  $\text{CH}_4$  have not often been measured in event plumes. The most comprehensive data set with respect to  $\text{H}_2$  and  $\text{CH}_4$  was collected from EP96A and EP96B at the Gorda Ridge in 1996 when  $\text{H}_2$  and  $\text{CH}_4$  concentrations reached maximum values of 47 and 7 nM, respectively (Kelley et al., 1998).

The generation of these voluminous plumes associated with magmatic events at the seafloor is not yet fully understood. To date, three different generation models have been proposed. The first model suggested that event plumes at the Cleft Segment, Juan de Fuca Ridge were generated through the sudden release of a crustal hydrothermal fluid reservoir by crustal rupture (Baker et al., 1989; Baker and Lupton, 1990; Lupton et al., 1999, 2000). A second model proposed event plume generation through the release of heat and chemical fluxes during a dike intrusion (Lowell and Germanovich, 1995). A third model postulates that event plumes form during interactions of seawater with emplaced lava flows or pillow lavas (Butterfield et al., 1997; Palmer and Ernst, 1998).

Based on physical and chemical data collected during the 2008 NELSC event plume, Baker et al. (2011) provided the first new clues on event plume formation in more than a decade. The study found that event plume volumes span over several orders of magnitude, the source fluid interacts with molten lava, and that the heat content in event plumes is roughly equivalent to that in the erupted lava. However, they also found that lava cooling is not fast enough to generate enough heat over short time to lift the plume up to 1000 m. Here we present further constraints on the NELSC event plume formation based on a more comprehensive chemical data set of the same event plume.

In the event plume over the NELSC eruption site, extraordinarily high  $\text{H}_2$  concentrations corresponded with nearly background  $^3\text{He}$  values. Thus, significant amounts of magmatic gases do not appear to be involved in the

formation of this event plume, consistent with previous event plume observations. As observed, Mn and Fe ascended together with H<sub>2</sub> in the plume released by this volcanic event. This is consistent with the results at Kilauea where both Mn and H<sub>2</sub> were abundant in the sea-surface eruptive plume (Sansone and Resing, 1995). Methane is present in low concentrations, is poorly correlated, and apparently decoupled from the other constituents in the shallow NELSC event plume.

Both the first and the second model suggest the release of a pre-existing hydrothermal fluid as a source fluid for the event plume. Our data is difficult to match to these models because of the very low and unsystematic CH<sub>4</sub> concentrations as well as the high H<sub>2</sub> values measured in the event plume. In contrast, the fluid chemistry data supports the third model, which suggests event plume generation during interaction of seawater with lava. This model is also consistent with the positive relationship between plume and lava heat (Baker et al., 2011). However, because the cooling rate of emplaced lava is argued to be too slow to generate enough buoyancy to lift the plume and much too slow to match the short release time of event plumes (Lavelle, 1995; Baker et al., 2011), other processes must occur during event plume formation. In the case at the NELSC, a process that releases enough heat in a short time is required to provide the required buoyancy flux for hydrothermal plume rise. Baker et al. (2011) argue that the amount of lava needed to interact with seawater to produce the high H<sub>2</sub> concentrations is relatively low and does not release enough heat to allow for the level of plume rise. Even if some of the lava exited as lava fountains, quenching of the pyroclastic material would not generate enough heat, if the mass fraction of pyroclasts is as low as, e.g., < 0.02% at Gorda Ridge, Escanaba Trough (Clague et al., 2009; Baker et al., 2011). However, glass shards that were commonly found in association with volcanic eruptions were discovered in the hydrothermal plumes at the NELSC. The shards together with the high H<sub>2</sub> concentrations could support the hypothesis that part of the lava emplacement was much more violent, probably similar to the West Mata eruptions, rather than just quiescent lava outflow. The larger surface area of lava available for interaction with seawater could have led to extensive H<sub>2</sub> production, possibly elevated cooling rates and only a minimum release of magmatic gas. Even though no evidence was found for a massive amount of pyroclastic debris, pyroclastic deposits were observed on the Puipui flow and on older proximate lava flows during ROV surveys in 2009 and their amounts could be underestimated. However, we still lack knowledge on event plume formation and the full extent of their generation processes remains unclear.

## CONCLUSION

1. The extremely high H<sub>2</sub> concentrations measured in the 2008 NELSC event plume confirm interaction of hot rock and seawater at the seafloor and point to an ongoing

eruption. Methane input is insignificant during event plume formation and rules out a mature, pre-stored fluid as fluid source. As observed in historical event plumes, significant amounts of magmatic gases do not appear to be involved in the formation of event plumes. The event plume chemistry favors a seawater-lava interaction formation model. However, the heat budget requires an additional process releasing enough heat to lift the plume within the short-lived event.

2. The extremely high H<sub>2</sub> concentrations in the event plume point to a large surface-area of hot-rock interacting with seawater and suggest that the Puipui eruption was locally more explosive than assumed, comparable to West Mata. This process might enhance the heat flux from lava cooling.
3. The near seafloor plume has a different source fluid than the event plume and likely results from the release of a more mature, pre-stored fluid rich in CH<sub>4</sub> and <sup>3</sup>He, either during event plume formation or shortly after.
4. The upper mantle is the main helium source of the NELSC eruption, similar to mid-ocean ridges.

## DATA AVAILABILITY STATEMENT

All chemical datasets generated for this study are included in the article and the **Supplementary Material**. Expedition reports for Lau Basin cruises in 2008, 2009, and 2010 can be downloaded at <http://www.pmel.noaa.gov/eoi/laubasin.html>. The CTD data is available at the Rolling Deck to Repository.

## AUTHOR CONTRIBUTIONS

TB wrote the manuscript made most of the figures, and analyzed CTD water samples for methane and hydrogen. ML was the lead PI for dissolved gases during the NE Lau 2008 expedition, analyzed CTD water samples for methane and hydrogen, and helped drafting this manuscript. JL was chief scientist on the NE Lau 2008 expedition and analyzed seawater samples for helium on shore. EB and SW collected and processed the CTD sensor data. JR and NB collected and analyzed seawater samples for manganese and iron. GF-G helped drafting the manuscript. All co-authors contributed to the interpretation of the results and to the editing of the manuscript.

## FUNDING

Support for this study was supplied by the NOAA Vents (now Earth-Ocean Interactions) Program, the Cooperative Institute for Marine Resources Studies (CIMRS) under NOAA Cooperative Agreement No. NA11OAR4320091, and the Joint

Institute for the Study of the Atmosphere and Ocean (JISAO) under NOAA Cooperative Agreement No. NA10OAR4320148. Financial support by the Swiss National Science Foundation grant #20MA21-115916 to GF-G was gratefully acknowledged. Funding for research cruises was provided by the U.S. National Science Foundation (NSF) and NOAA Office of Ocean Exploration and Research. This is PMEL contribution 4943.

## ACKNOWLEDGMENTS

We thank the crew and technical staff of the research vessel *T.G. Thompson* and the ROV *Jason* team for excellent support during our expeditions. We thank Ron Greene, Leigh Evans, and Hoang-My Christensen for assistance with sampling and analyses and

Susan Merle for creating the bathymetric map in **Figure 1**. The manuscript was improved by the helpful comments from the two reviewers and the Topic Editors.

## SUPPLEMENTARY MATERIAL

The Supplementary Material for this article can be found online at: <https://www.frontiersin.org/articles/10.3389/fmars.2020.00171/full#supplementary-material>

**TABLE S1** | Summary of concentrations of H<sub>2</sub>, CH<sub>4</sub>, [<sup>3</sup>He]<sup>A</sup>, TDMn, and TDFe and ratios thereof in the event, near seafloor and deep plumes above the Puipui eruption site in 2008, 2009, and 2010 and in the background waters of the eruption site.

## REFERENCES

- Amend, J. P., McCollom, T. M., Hentscher, M., and Bach, W. (2011). Catabolic and anabolic energy for chemolithoautotrophs in deep-sea hydrothermal systems hosted in different rock types. *Geochim. Cosmochim. Acta* 75, 5736–5748. doi: 10.1016/j.gca.2011.07.041
- Anantharaman, K., Breier, J. A., Sheik, C. S., and Dick, G. J. (2013). Evidence for hydrogen oxidation and metabolic plasticity in widespread deep-sea sulfur-oxidizing bacteria. *Proc. Natl. Acad. Sci. U.S.A.* 110, 330–335. doi: 10.1073/pnas.1215340110
- Baker, E. T. (1998). Patterns of event and chronic hydrothermal venting following a magmatic intrusion: new perspectives from the 1996 Gorda Ridge eruption. *Deep Sea Res. Pt. II* 45, 2599–2618. doi: 10.1016/S0967-0645(98)00085-X
- Baker, E. T., German, C. R., and Elderfield, H. (1995a). “Hydrothermal plumes over spreading-center axes: global distributions and geological inferences,” in *Seafloor Hydrothermal Systems: Physical, Chemical, Biological, and Geological Interactions*, eds S. E. Humphris, et al. (Washington, DC: American Geophysical Union), 47–71. doi: 10.1029/gm091p0047
- Baker, E. T., Lavelle, J. W., Feely, R. A., Massoth, G. J., Walker, S. L., and Lupton, J. E. (1989). Episodic venting of hydrothermal fluids from the Juan de Fuca ridge. *J. Geophys. Res.* 94, 9237–9250. doi: 10.1029/JB094iB7p09237
- Baker, E. T., and Lupton, J. E. (1990). Changes in submarine hydrothermal He-3/heat ratios as an indicator of magmatic tectonic activity. *Nature* 346, 556–558. doi: 10.1038/346556a0
- Baker, E. T., Lupton, J. E., Resing, J. A., Baumberger, T., Lilley, M. D., Walker, S. L., et al. (2011). Unique event plumes from a 2008 eruption on the Northeast Lau Spreading center. *Geochem. Geophys. Geosyst.* 12:Q0AF02. doi: 10.1029/2011GC003725
- Baker, E. T., Massoth, G. J., and Feely, R. A. (1987). Cataclysmic hydrothermal venting on the Juan-de-Fuca ridge. *Nature* 329, 149–151. doi: 10.1038/329149a0
- Baker, E. T., Massoth, G. J., Feely, R. A., Embley, R. W., Thomson, R. E., and Burd, B. J. (1995b). Hydrothermal event plumes from the CoAxial seafloor Eruption Site, Juan de Fuca Ridge. *Geophys. Res. Lett.* 22, 147–150. doi: 10.1029/94GL02403
- Baumberger, T., Lilley, M. D., Resing, J. A., Lupton, J. E., Baker, E. T., Butterfield, D. A., et al. (2014). Understanding a submarine eruption through time series hydrothermal plume sampling of dissolved and particulate constituents: West Mata, 2008–2012. *Geochem. Geophys. Geosyst.* 15, 4631–4650. doi: 10.1002/2014GC005460
- Bennett, S. A., Achterberg, E. P., Connelly, D. P., Statham, P. J., Fones, G. R., and German, C. R. (2008). The distribution and stabilization of dissolved Fe in deep-sea hydrothermal plumes. *Earth Planet. Sci. Lett.* 270, 157–167. doi: 10.1016/j.epsl.2008.01.048
- Bowers, T. S., Campbell, A. C., Measures, C. I., Spivack, A. J., Khadem, M., and Edmond, J. E. (1988). Chemical controls on the composition of vent fluids at 13° - 11°N, and 21°N, East Pacific Rise. *J. Geophys. Res.* 93, 4522–4536. doi: 10.1029/JB093iB05p04522
- Buck, N. J., Resing, J. A., Baker, E. T., and Lupton, J. E. (2018). Chemical fluxes from a recently erupted shallow submarine volcano on the Mariana Arc. *Geochem. Geophys. Geosyst.* 19, 1660–1673. doi: 10.1029/2018GC007470
- Butterfield, D. A., Jonasson, I. R., Massoth, G. J., Feely, R. A., Roe, K. K., Embley, R. E., et al. (1997). Seafloor eruptions and evolution of hydrothermal fluid chemistry. *Philos. Trans. R. Soc. Lond.* 355, 369–386. doi: 10.1098/rsta.1997.0013
- Butterfield, D. A., Nakamura, K., Takano, B., Lilley, M. D., Lupton, J. E., Resing, J. A., et al. (2011). High SO<sub>2</sub> flux, sulfur accumulation and gas fractionation at an erupting submarine volcano. *Geology* 39, 803–806. doi: 10.1130/G31901.1
- Butterfield, D. A., Roe, K. K., Lilley, M. D., Huber, J. A., Baross, J. A., Embley, R. W., et al. (2004). “Mixing, Reaction and Microbial activity in the sub-seafloor revealed by temporal and spatial variation in diffuse flow vents at axial volcano,” in *The Subseafloor Biosphere at Mid-Ocean Ridges*, eds W. S. D. Wilcock, et al. (Washington, DC: American Geophysical Union), 269–289. doi: 10.1029/144gm17
- Chadwick, W. W. Jr., Cashman, K. V., Embley, R. W., Matsumoto, H., and Dziak, R. P. (2008). Direct video and hydrophone observations of submarine explosive eruptions at NW Rota-1 Volcano, Mariana Arc. *J. Geophys. Res.* 113:B08S10. doi: 10.1029/2007JB005215
- Chadwick, W. W. Jr., Merle, S. G., Baker, E. T., Walker, S. L., Resing, J. A., Butterfield, D. A., et al. (2018). A recent volcanic eruption discovered on the central Mariana back-arc spreading center. *Front. Earth Sci.* 6:172. doi: 10.3389/feart.2018.00172
- Chadwick, W. W. Jr., Rubin, K. H., Merle, S. G., Bobbitt, A. M., Kwasnitschka, T., and Embley, R. W. (2019). Recent eruptions between 2012–2018 discovered at West Mata submarine volcano (NE Lau Basin, SW Pacific) and characterized by new ship, AUV, and ROV data. *Front. Mar. Sci.* 6:495. doi: 10.3389/fmars.2019.00495
- Clague, D. A., Caress, D. W., Rubin, K. H., and Paduan, J. B. (2010). The 2008 puipui eruption and morphology of the northeast Lau spreading center between Maku and Tafu. *Paper Presented at the 2010 AGU Fall Meeting*, San Francisco, CA.
- Clague, D. A., Paduan, J. B., and Davis, A. S. (2009). Widespread strombolian eruptions of mid-ocean ridge basalt. *J. Volcanol. Geotherm. Res.* 180, 171–188. doi: 10.1016/j.jvolgeores.2008.08.007
- de Angelis, M. A., Lilley, M. D., and Baross, J. (1993). Methane oxidation in deep-sea hydrothermal plumes of the Endeavour segment of the Juan de Fuca Ridge. *Deep Sea Res. Pt. I* 40, 1169–1186. doi: 10.1016/0967-0637(93)90132-M
- Dick, G. J. (2019). The microbiomes of deep-sea hydrothermal vents: distributed globally, shaped locally. *Nat. Rev. Microbiol.* 17, 271–283. doi: 10.1038/s41579-019-0160-2
- Dick, G. J., Anantharaman, K., Baker, B. J., Li, M., Reed, D. C., and Sheik, C. S. (2013). The microbiology of deep-sea hydrothermal vent plumes: ecological and biogeographic linkages to seafloor and water column habitats. *Front. Microbiol.* 4:124. doi: 10.3389/fmicb.2013.00124

- Embley, R. W., Chadwick, W. W. Jr., Jonasson, I. R., Butterfield, D. A., and Baker, E. T. (1995). Initial results of the rapid response to the 1993 CoAxial event: relationships between hydrothermal and volcanic processes. *Geophys. Res. Lett.* 22, 143–146. doi: 10.1029/94GL02281
- Embley, R. W., Merle, S. G., Baker, E. T., Rubin, K. H., Lupton, J. E., Resing, J. A., et al. (2014). Eruptive modes and hiatus of volcanism at West Mata seamount, NE Lau basin: 1996–2012. *Geochem. Geophys. Geosyst.* 15, 4093–4115. doi: 10.1002/2014GC005387
- Embley, R. W., and Rubin, K. H. (2018). Extensive young silicic volcanism produces large deep submarine lava flow in the NE Lau Basin. *Bull. Volcanol.* 80:36.
- Field, M. P., and Sherrell, R. M. (2000). Dissolved and particulate Fe in a hydrothermal plume at 9° 45'N, East Pacific Rise: slow Fe (II) oxidation kinetics in Pacific plumes. *Geochim. Cosmochim. Acta.* 64, 619–628. doi: 10.1016/S0016-7037(99)00333-6
- Fourre, E., Jean-Baptiste, P., Charlou, J.-L., Donval, J. P., and Ishibashi, J. I. (2006). Helium Isotope composition of hydrothermal fluids from the Manus back-arc Basin, Papua New Guinea. *Geochem. J.* 40, 245–252. doi: 10.2343/geochemj.40.245
- German, C. R., Baker, E. T., Connelly, D. P., Lupton, J. E., Resing, J. A., Prien, R. D., et al. (2006). Hydrothermal exploration of the fonualei rift and spreading center and the northeast lau spreading center. *Geochem. Geophys. Geosyst.* 7:Q11022. doi: 10.1029/2006GC001324
- Graham, D. W. (2002). “Noble gas isotope geochemistry of mid-ocean ridge and ocean island basalts; characterization of mantle sources reservoirs,” in *Noble Gases in Geochemistry and Cosmochemistry*, eds D. Porcelli, R. Wieler, and C. Ballantine, (Washington, DC: Mineralogical Society of America), 247–318. doi: 10.1515/9781501509056-010
- Graham, D. W., Michael, P. J., and Rubin, K. H. (2018). An investigation of mid-ocean ridge degassing using He, CO<sub>2</sub>, and δ<sup>13</sup>C variations during the 2005–06 eruption at 9°50'N on the East Pacific Rise. *Earth Planet. Sci. Lett.* 504, 84–93. doi: 10.1016/j.epsl.2018.09.040
- Hawkins, J. W. (1995). “Evolution of the lau basin - insights from ODP leg 135,” in *Active Margins and Marginal Basins of the Western Pacific*, eds B. Taylor, and J. Natland, (Washington, DC: American Geophysical Society), 125–173. doi: 10.1029/gm088p0125
- Hilton, D. R., Fisher, T. P., and Marty, B. (2002). Noble gases and volatile recycling at subduction zones. *Rev. Mineral. Geochem.* 47, 319–370. doi: 10.1515/9781501509056-011
- Huber, J. A., Butterfield, D. A., and Baross, J. A. (2003). Bacterial diversity in a subsurface habitat following a deep-sea volcanic eruption. *FEMS Microbiol. Ecol.* 43, 393–409. doi: 10.1111/j.1574-6941.2003.tb01080.x
- Kelley, D. S., Lilley, M. D., Lupton, J. E., and Olsen, E. J. (1998). Enriched H<sub>2</sub>, CH<sub>4</sub> and 3He concentrations in hydrothermal plumes associated with the 1996 Gorda Ridge eruptive event. *Deep Sea Res. Pt. II* 45, 2665–2682. doi: 10.1016/S0967-0645(98)00088-5
- Kim, J., Son, S. K., Son, J. W., Kim, K. H., Shim, W. J., Kim, C. H., et al. (2009). Venting sites along the fonualei and Northeast lau spreading centers and evidence of hydrothermal activity at an off-axis caldera in the northeastern lau basin. *Geochem. J.* 43, 1–13. doi: 10.2343/geochemj.01164
- Lavelle, J. W. (1995). The initial rise of a hydrothermal plume from a line segment source - results from a three-dimensional numerical model. *Geophys. Res. Lett.* 22, 159–162. doi: 10.1029/94GL01463
- Lilley, M. D., Butterfield, D. A., Lupton, J. E., and Olsen, E. J. (2003). Magmatic events can produce rapid changes in hydrothermal vent chemistry. *Nature* 422, 878–881. doi: 10.1038/nature01569
- Lilley, M. D., Feely, R. A., and Treffy, J. H. (1995). “Chemical and biological transformations in hydrothermal plumes,” in *Seafloor Hydrothermal Systems: Physical, Biological, and Geological Interactions*, eds S. E. Humphris, et al. (Washington, D.C: American Geophysical Union), 369–391. doi: 10.1029/gm091p0369
- Lowell, R. P., and Germanovich, L. N. (1995). Dike injection and the formation of megaplumes at ocean ridges. *Science* 267, 1804–1807. doi: 10.1126/science.267.5205.1804
- Lupton, J. E. (1995). “Hydrothermal plumes: near and far field,” in *Seafloor Hydrothermal Systems: Physical, Chemical, Biological, and Geological Interactions*, eds S. E. Humphris, et al. (Washington, DC: American Geophysical Union), 317–346. doi: 10.1029/gm091p0317
- Lupton, J. E., Baker, E. T., and Massoth, G. J. (1989). Variable 3He/heat ratios in submarine hydrothermal systems: evidence from two plumes over the Juan de Fuca ridge. *Nature* 337, 161–164. doi: 10.1038/337161a0
- Lupton, J. E., Baker, E. T., and Massoth, G. J. (1999). Helium, heat, and the generation of hydrothermal event plumes at mid-ocean ridges. *Earth Planet. Sci. Lett.* 171, 343–350. doi: 10.1016/S0012-821X(99)00149-1
- Lupton, J. E., Baker, E. T., and Massoth, G. J. (2000). Reply to Comment on “Helium, heat and the generation of hydrothermal event plumes at mid-ocean ridges”, by J.E. Lupton, E.T. Baker and G.J. Massoth. *Earth Planet. Sci. Lett.* 180, 219–222. doi: 10.1016/S0012-821X(00)00151-5
- Lupton, J. E., Baker, E. T., Massoth, G. J., Thomson, R. E., Burd, B. J., Butterfield, D. A., et al. (1995). Variations in water-column 3He/heat ratios associated with the 1993 CoAxial event, Juan de Fuca ridge. *Geophys. Res. Lett.* 22, 155–158. doi: 10.1029/94GL02797
- Lupton, J. E., Rubin, K. H., Arculus, R., Lilley, M. D., Butterfield, D. A., Resing, J. A., et al. (2015). Helium isotope, C/3He, and Ba-Nb-Ti signatures in the northern Lau Basin: distinguishing arc, back-arc, and hotspot affinities. *Geochem. Geophys. Geosyst.* 16, 1133–1155. doi: 10.1002/2014GC005625
- McCollom, T. M. (2000). Geochemical constraints on primary productivity in submarine hydrothermal vent plumes. *Deep Sea Res. Pt. I* 47, 85–101. doi: 10.1016/S0967-0637(99)00048-5
- McCollom, T. M., and Shock, E. L. (1997). Geochemical constraints on chemolithoautotrophic metabolism by microorganisms in seafloor hydrothermal systems. *Geochim. Cosmochim. Acta* 61, 4375–4391. doi: 10.1016/S0016-7037(97)00241-X
- McLaughlin, E. A. (1998). *Microbial Hydrogen Oxidation Associated With Deep-sea Hydrothermal Vent Environments*. Ph.D. dissertation, University of Washington, Seattle, WA.
- McLaughlin, E. A., Lilley, M. D., Olsen, E. J., and Rust, T. (1996). Microbial hydrogen oxidation in the Loihi event plumes: microbial rapid response. *Eos Trans. Am. Geophys. Union* 46:398.
- McLaughlin-West, E. A., Olson, E. J., Lilley, M. D., Resing, J. A., Lupton, J. E., Baker, E. T., et al. (1999). Variations in hydrothermal methane and hydrogen concentrations following the 1998 eruption at Axial Volcano. *Geophys. Res. Lett.* 26, 3453–3456. doi: 10.1029/1999GL002336
- Measures, C. I., Yuan, J., and Resing, J. A. (1995). Determination of iron in seawater by flow injection analysis using in-line preconcentration and spectrophotometric detection. *Mar. Chem.* 50, 3–12. doi: 10.1016/0304-4203(95)00022-J
- Mottl, M. J., Sansone, F. J., Wheat, C. G., Resing, J. A., Baker, E. T., and Lupton, J. E. (1995). Manganese and methane in hydrothermal plumes along the east pacific rise, 8°40' to 11°50'N. *Geochim. Cosmochim. Acta* 59, 4147–4165. doi: 10.1016/0016-7037(95)00245-U
- Nojiri, Y., Ishibashi, J., Kawai, T., and Sakai, H. (1989). Hydrothermal plumes along the north fiji basin spreading axis. *Nature* 342, 667–670. doi: 10.1038/342667a0
- Palmer, M. R., and Ernst, G. G. J. (1998). Generation of hydrothermal megaplumes by cooling of pillow basalts at mid-ocean ridges. *Nature* 393, 643–647. doi: 10.1038/31397
- Poreda, R., and Craig, H. (1989). Helium isotope ratios in Circum Pacific volcanic arcs. *Nature* 473–478. doi: 10.1038/338473a0
- Resing, J. A., Baker, E. T., Lupton, J. E., Walker, S. L., Butterfield, D. A., Massoth, G. J., et al. (2009). Chemistry of the hydrothermal plumes above submarine volcanoes of the Mariana Arc. *Geochem. Geophys. Geosyst.* 10:Q02009. doi: 10.1029/2008GC002141
- Resing, J. A., Lebon, G., Baker, E. T., Lupton, J. E., Embley, R. W., Massoth, G. J., et al. (2007). Venting of acid-sulfate fluids in a high-sulfidation setting at NW Rota-1 submarine volcano on the Mariana Arc. *Econ. Geol.* 102, 1047–1061. doi: 10.2113/gsecongeo.102.6.1047
- Resing, J. A., and Mottl, M. J. (1992). Determination of manganese in seawater using flow injection analysis with on-line preconcentration and spectrophotometric detection. *Anal. Chem.* 64, 2682–2687. doi: 10.1021/ac00046a006
- Resing, J. A., Rubin, K. H., Embley, R. W., Lupton, J. E., Baker, E. T., Dziak, R. P., et al. (2011). Active submarine eruption of boninite in the northeast Lau Basin. *Nat. Geosci.* 4, 799–806. doi: 10.1038/NGEO1275
- Resing, J. A., Sedwick, P. N., German, C. R., Jenkins, W. J., Moffett, J. W., Sohst, B. M., et al. (2015). Basin-scale transport of hydrothermal dissolved metals across the South Pacific Ocean. *Nature* 523, 200–203. doi: 10.1038/nature14577

- Rubin, K. H., Embley, R. W., Clague, D. A., Resing, J. A., Michael, P. J., Keller, N. S., et al. (2009). Lavas from active boninite and very recent basalt eruptions at two submarine NE Lau basin sites. *Paper Presented at the 2009 AGU Fall Meeting*, San Francisco, CA.
- Rubin, K. H., Soule, S. A., Chadwick, W. W. Jr., Fornari, D. J., and Clague, D. A. (2012). Volcanic eruptions in the deep sea. *Oceanography* 25, 142–157. doi: 10.5670/oceanog.2012.12
- Sander, S. G., and Koschinsky, A. (2011). Metal flux from hydrothermal vents increased by organic complexation. *Nat. Geosci.* 4, 145–150. doi: 10.1038/NGEO1088
- Sansone, F. J., and Resing, J. A. (1995). Hydrography and geochemistry of sea-surface hydrothermal plumes resulting from Hawaiian coastal volcanism. *J. Geophys. Res.* 100, 13555–13569.
- Sansone, F. J., Resing, J. A., Tribble, G. W., Sedwick, P. N., Kelley, K. M., and Hon, K. (1991). Lava-seawater interactions at shallow-water submarine lava flows. *Geophys. Res. Lett.* 18, 1731–1734. doi: 10.1029/91GL01279
- Stern, R. J., Tamura, Y., Embley, R. W., Ishizuka, O., Merle, S., Basu, N. K., et al. (2008). Evolution of West Rota Volcano, an extinct submarine volcano in Southern Mariana Arc: evidence from sea floor morphology, remotely operated vehicle observations, and <sup>40</sup>Ar-<sup>39</sup>Ar geochronological studies. *Isl. Arc.* 17, 70–89. doi: 10.1111/j.1440-1738.2007.00600.x
- Von Damm, K. L. (1990). Seafloor hydrothermal activity: black smoker chemistry and chimneys. *Annu. Rev. Earth Planet. Sci.* 18, 173–204. doi: 10.1146/annurev.ea.18.050190.001133
- Von Damm, K. L., and Lilley, M. D. (2004). “Diffuse flow hydrothermal fluids from 9° 50' N East Pacific Rise: origin, evolution and biogeochemical controls,” in *The Subseafloor Biosphere at Mid-Ocean Ridges*, eds W. S. D. Wilcock, et al. (Washington, DC: American Geophysical Union), 245–268. doi: 10.1029/144gm16
- Welhan, J. A. (1988). Origins of methane in hydrothermal systems. *Chem. Geol.* 71, 183–198. doi: 10.1016/0009-2541(88)90114-3
- Xu, G., Chadwick, W. W. Jr., Wilcock, W. S. D., Bemis, K. G., and Delaney, J. (2018). Observation and modeling of hydrothermal response to the 2015 Eruption at Axial Seamount, Northeast Pacific. *Geochem. Geophys. Geosyst.* 19, 2780–2797. doi: 10.1029/2018GC007607
- Young, C., and Lupton, J. E. (1983). An ultra-tight fluid sampling system using cold-welded copper tubing. *Eos Trans. Am. Geophys. Union* 64:735.
- Yücel, M., Gartman, A., Chan, C. S., and Luther, G. W. III (2011). Hydrothermal vents as a kinetically stable source of iron-sulphide-bearing nanoparticles to the ocean. *Nat. Geosci.* 4, 367–371. doi: 10.1038/NGEO1148
- Zellmer, K. E., and Taylor, B. (2001). A three-plate kinematic model for Lau Basin opening. *Geochem. Geophys. Geosyst.* 2:1020. doi: 10.1029/2000GC000106
- Conflict of Interest:** The authors declare that the research was conducted in the absence of any commercial or financial relationships that could be construed as a potential conflict of interest.
- Copyright © 2020 Baumberger, Lilley, Lupton, Baker, Resing, Buck, Walker and Früh-Green. This is an open-access article distributed under the terms of the Creative Commons Attribution License (CC BY). The use, distribution or reproduction in other forums is permitted, provided the original author(s) and the copyright owner(s) are credited and that the original publication in this journal is cited, in accordance with accepted academic practice. No use, distribution or reproduction is permitted which does not comply with these terms.